Mater. Res. Soc. Symp. Proc. Vol. 1642 © 2014 Materials Research Society
DOI: 10.1557/opl.2014.443

# Integrated Thermoelectric–Thermal System Resistance Optimization to Maximize Power Output in Thermoelectric Energy Recovery Systems

Terry J. Hendricks*
National Aeronautics & Space Administration – Jet Propulsion Laboratory
Power and Sensors Section, Thermal Energy Conversion Technology
Pasadena, CA 91109

## ABSTRACT

Thermoelectric energy recovery is an important technology for recovering waste thermal energy in high-temperature industrial, transportation and military energy systems. Thermoelectric (TE) power systems in these applications require high performance hot-side and cold-side heat exchangers to provide the critical temperature differential and transfer the required thermal energy to create the power output. Hot-side and cold-side heat exchanger performance is typically characterized by hot-side and cold-side thermal resistances, $R_{h,th}$ and $R_{c,th}$, respectively. Heat exchanger performance determines the hot-side temperature, $T_h$, and cold-side temperature, $T_c$, conditions when operating in energy recovery environments with available temperature differentials characterized by exhaust temperatures, $T_{exh}$, and ambient temperature, $T_{amb}$. This work analytically defined a crucially important design relationship between ($P/P_{max}$) and ($R_{h,th}$ / $R_{c,th}$) in TE power generation systems to determine the optimum ratio of ($R_{h,th}$ / $R_{c,th}$) maximizing TE system power. A sophisticated integrated TE device / heat exchanger analysis was used, which simultaneously integrates hot- and cold-side heat exchanger models with TE device optimization models incorporating temperature-dependent TE material properties for p-type and n-type materials, thermal and electrical contact resistances, and hot side and cold side heat loss factors. This work examined the ($P/P_{max}$) - ($R_{h,th}$ / $R_{c,th}$) relationship for system designs employing single-material and segmented-material TE couple legs with various TE material combinations, including bismuth telluride alloys, skutterudite compounds, and skutterudite / bismuth telluride segmented combinations. This work defined the non-dimensional functional relationships and found the optimum thermal resistance condition:

$$(R_{h,th} / R_{c,th})_{opt} > 10 \text{ to } 30$$

created the maximum power output in TE optimized designs for various TE material combinations investigated. The non-dimensional relationships were investigated for various electrical contact resistances, differing thermal loss factors, and at various hot-side/cold-side temperature conditions. This work showed that the non-dimensional functional relationships were invariant under these differing conditions. It was determined that a condition of ($R_{h,th}$ / $R_{c,th}$) = 1 creates power output far below maximum power conditions. The ($P/P_{max}$) - ($R_{h,th}$ / $R_{c,th}$) relationship also dictated certain temperature profile conditions, defined by the parameter, ($T_h - T_c$) / ($T_{exh} - T_{amb}$), which were directly associated with design points in this relationship including maximum power points. The value of ($T_h - T_c$) / ($T_{exh} - T_{amb}$) was generally less than 0.5 at maximum power conditions in TE energy recovery designs using TE materials investigated here. The wide-ranging ramifications on TE energy recovery systems and their design optimization for industrial and transportation-related applications are discussed.

*Corresponding Author e-mail: terry.j.hendricks@jpl.nasa.gov Phone: 1-818-354-4779
Address: 4800 Oak Grove Drive, Pasadena, CA 91109-8099

## INTRODUCTION

Various transportation vehicles (commercial and military) and industrial process systems create and dissipate enormous amounts of waste thermal energy globally every year. Multiple Quads (1 Quad = $10^{15}$ Btu) are dissipated annually in the United States alone [1-3]. Thermoelectric (TE) energy recovery and conversion systems is an important technology for recovering this waste thermal energy and converting it to useful electrical energy, either by itself or as a critical energy conversion subsystem in a hybrid power system. Various research and development projects have investigated, designed and developed advanced TE materials and systems to recovery thermal energy in high-temperature industrial, transportation, and military energy systems [3-12]. Thermoelectric (TE) power systems in these applications require high performance hot-side and cold-side heat exchangers to provide the critical temperature differential and transfer the required thermal energy to create the power output. In order to achieve the maximum power output these TE power systems must undergo sophisticated TE design optimization [13, 14] that is tightly integrated and coupled with thermal system optimization [5, 6, 11, 12, 14, 15]. Thermoelectric (TE) power systems in these applications require high performance hot-side and cold-side heat exchangers to provide the critical temperature differential and transfer the required thermal energy to create the power output. Hot-side and cold-side heat exchanger performance is typically characterized by hot-side and cold-side thermal resistances, $R_{h,th}$ and $R_{c,th}$, respectively, and it is critical to know the relationship between $R_{h,th}$ and $R_{c,th}$ which maximizes power output. Yazawa and Shakouri [16] attempted to address this question with a simplified, closed-form analysis of the quite complex thermal and thermoelectric design interactions described in earlier references [3-15]. This work leverages the complex, integrated thermal/thermoelectric analyses described in Hendricks et al. [11, 12, 14, 15] to provide a more complete picture and illuminate the critical subtleties in determining the optimum $R_{h,th}$ / $R_{c,th}$ relationship that maximizes power output in TE energy recovery systems. This work was able to identify the critical optimum ($R_{h,th}$ / $R_{c,th}$) values and identify some unique (P / $P_{max}$) versus ($R_{h,th}$ / $R_{c,th}$) relationships that help to define the optimum values.

## DESIGN OPTIMIZATION METHODOLOGY

A sophisticated integrated TE device / heat exchanger analysis was used, which simultaneously integrates hot- and cold-side heat exchanger models with TE device optimization models incorporating temperature-dependent TE material properties for p-type and n-type materials, thermal and electrical contact resistances, and hot side and cold side heat loss factors. This integrated analysis is defined in Hendricks et al. [11, 12, 14, 15]. Figure 1 schematically shows the integrated heat exchanger/TE device model used in this analysis. The TE device shown schematically in Figure 1 is nominally a multiple couple device employing either single p-type and n-type materials in each couple or a segmented p-type and n-type design in each couple (as shown in Figure 1). The hot-side and cold-side heat exchanger designs are nominally gas or liquid exchanger designs implementing various configurations that are compatible with satisfying heat flux requirements with the TE devices (i.e., interface heat flux matching). The hot-side and cold-side thermal designs providing the necessary heat transfer are characterized by the $R_{h,th}$ and $R_{c,th}$, respectively, shown in Figure 1, which represent the series summation of all the thermal resistances

*Corresponding Author e-mail: terry.j.hendricks@jpl.nasa.gov Phone: 1-818-354-4779
Address: 4800 Oak Grove Drive, Pasadena, CA 91109-8099

between the heat exchange fluid and the TE device hot- or cold-side interfaces operating at $T_h$ and $T_c$, respectively, described by equations 1 and 2. $R_{h,th,i}$ are all the individual thermal resistances at the TE device hot-side, while $R_{c,th,i}$ are all the corresponding individual thermal resistances at the TE device cold-side.

$$R_{h,th} = \sum_i R_{h,th,i} \quad (1)$$

$$R_{c,th} = \sum_i R_{c,th,i} \quad (2)$$

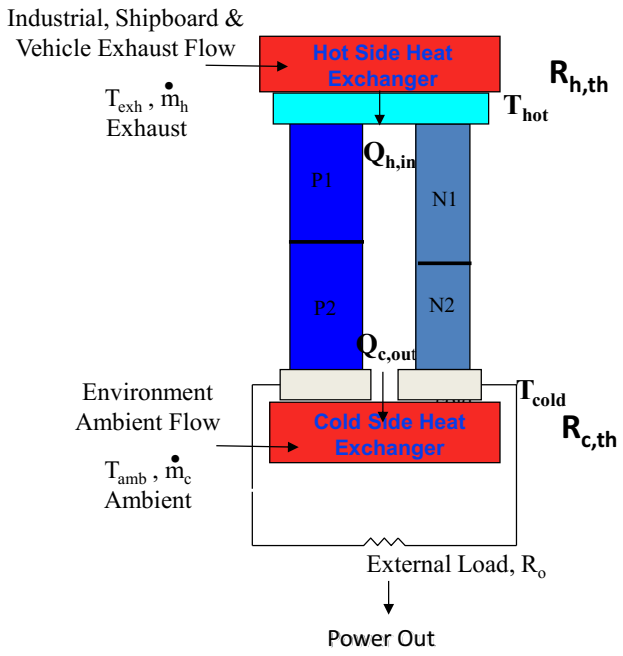


**Figure 1.** Schematic Representation of the Heat Exchanger/TE Device System with Appropriate Heat Flows and Hot-Side and Cold-Side Thermal Resistances.

The hot-side heat flows, temperatures and thermal resistances and cold-side heat flows, temperatures, and thermal resistances are typically related by mathematical expressions given by Hendricks et al. [11, 12, 14, 15], but not replicated here for brevity. Hendricks et al. [14, 15] describes how this system analysis approach is used to define critical maximum efficiency-power maps that define the loci of all possible TE designs and their power and conversion efficiency for a given $T_{exh}$, $T_{amb}$, $\dot{m}_h$ , and $UA_h$. The maximum efficiency – power map (See Figure 2) defines the tradeoff between maximum efficiency and power output for the various designs possible in a given application, and they define the maximum power point (MPME) that can be achieved resulting from the complex heat exchanger – TE device interaction and interdependencies in a design application. In addition, at each point of the maximum efficiency – power map (Figure 2) one knows the hot-side and cold-side heat flows, temperature conditions, and the specific TE device design such as number of couples and TE couple dimensions. A common question and need is to know in any given TE energy recovery power system design is what is the optimum selection of $R_{h,th}$ and $R_{c,th}$ to maximize power output. A related critical question is the relationship between the TE device temperature differential, $(T_h - T_c)$, and the overall system temperature, $(T_{exh} - T_{amb})$, at the optimum selection of $R_{h,th}$ and $R_{c,th}$.

*Corresponding Author e-mail: terry.j.hendricks@jpl.nasa.gov Phone: 1-818-354-4779
Address: 4800 Oak Grove Drive, Pasadena, CA 91109-8099

This work has addressed this question by using non-dimensional analysis, the design optimization techniques described in Hendricks et al. [11, 12, 14, 15], and investigating the normalized power – thermal resistance ratio domain space for different TE material combinations and TE system design parameters. Using non-dimensional analysis techniques, one can characterize the normalized power - thermal resistance relationship as given in equation 3.

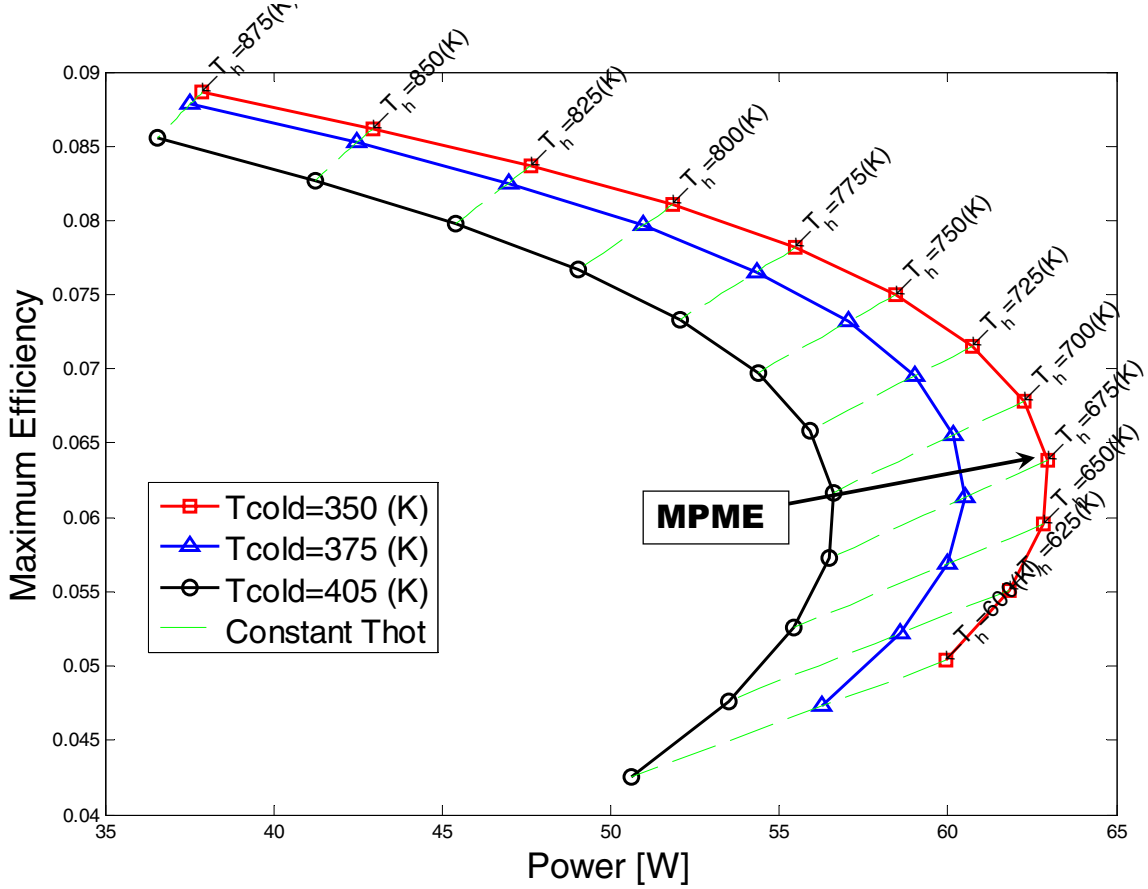


**Figure 2.** Maximum Efficiency – Power Output Map for Different Hot-side Temperatures, Cold-Side Temperatures, Exhaust Temperature of 1023 K, and Ambient Temperature 300 K.

Additionally, one can characterize the device temperature differential – system temperature differential as given in equation 4. This work will show that these relationships are unique for a given selection of TE material properties across a wide range of design parameters. Not only are

$$\left(\frac{P}{P_{\max}}\right) = f\left[\left(\frac{R_{h,th}}{R_{c,th}}\right), TE \cdot Material \cdot \Pr operties\right] \tag{3}$$

$$\left(\frac{T_h - T_c}{T_{exh} - T_{amb}}\right) = f\left[\left(\frac{R_{h,th}}{R_{c,th}}\right), TE \cdot Material \cdot \Pr operties\right] \tag{4}$$

*Corresponding Author e-mail: terry.j.hendricks@jpl.nasa.gov Phone: 1-818-354-4779
Address: 4800 Oak Grove Drive, Pasadena, CA 91109-8099

these relationships unique, but once these relationships are quantified they demonstrate and elucidate the proper optimum selection of $[R_{h,th}/R_{c,th}]$ which results in global maximum power in a given TE energy recovery system design.

The design optimization techniques shown in Hendricks and Crane [14], Hendricks [15], and typical analytic results shown in Figure 2 were used in this investigation to determine the optimum power points (i.e., MPME) for any given selection of $R_{h,th}$ , $R_{c,th}$, and therefore $[R_{h,th}/R_{c,th}]$ ratio. The optimum power points were then surveyed to determine and establish the $[P/P_{max}]$ relationship shown in equation 3. Simultaneously, one could also determine the value of $[(T_h - T_c)/(T_{exh} - T_{amb})]$ at the optimum power points for a given selection of $R_{h,th}$ , $R_{c,th}$, and therefore $[R_{h,th}/R_{c,th}]$ ratio and establish the relationship given in equation 4.

## RESULTS AND DISCUSSION

Several TE system design cases were investigated in this analytical system study for a typical energy recovery application where $T_{exh}$ = 1023 K and $T_{amb}$ = 300 K. This is a condition that is common to certain industrial process energy recovery applications and even fuel cell systems. The TE system design cases were investigated using three different sets of TE materials:

Set 1 - An n-type and p-type Skutterudite material combination in a single-material TE couple design (i.e., one material in each couple leg),

Set 2 – An n-type Skutterudite / n-type Bismuth Telluride and p-type Skutterudite / p-type Bismuth Telluride material combination in a dual-segmented TE couple design (i.e., two separate materials in each couple leg), and

Set 3 – An n-type Bismuth Telluride and p-type Bismuth Telluride material combination in a single-material TE couple design (i.e., one material in each couple leg).

The n-type and p-type Skutterudite materials used were similar to those developed and reported on by the National Aeronautics and Space Administration (NASA) – Jet Propulsion Laboratory and others in the mid-2000's [17-20]. The bismuth telluride materials used were similar to those developed and reported on in the literature dating back to the 1980's-1990's [17, 21]. The choice of materials used was not the focus of this investigation as several different TE material types could be chosen in concentrating on the TE system design aspects discussed herein. The point was to use sufficiently different material sets such that one could draw system-level design conclusions that incorporated effects of material selections within the constraints of their typical operational and measured temperature ranges. In particular, this work was interested in the differences of single-material couple designs and dual-segmented coupled designs.

The power output, P, at the MPME point in Figure 2 was characterized for different values of $R_{h,th}$ , $R_{c,th}$, and $[R_{h,th}/R_{c,th}]$ ratio for these two material selections in this analytic investigation. The MPME power output was then compared with the global maximum power, $P_{max}$, determined from the various $R_{h,th}$ , $R_{c,th}$, and $[R_{h,th}/R_{c,th}]$ ratio cases studied. Figure 3 shows the resulting $[P/P_{max}]$ relationship as a function of $[R_{h,th}/R_{c,th}]$ discovered in this investigation for these two selected material sets. The data reveals that $[P/P_{max}]$ increases smoothly and rapidly as $[R_{h,th}/R_{c,th}]$ increases, until $[P/P_{max}]$ asymptotes to 1 at relatively large values of $[R_{h,th}/R_{c,th}]$. The exact $[P/P_{max}]$ - $[R_{h,th}/R_{c,th}]$ relationship is dependent on the TE materials selected, but in all the cases studied, which varied $R_{h,th}$ across at least two orders of magnitude, these relationships held. As $R_{h,th}$ was decreased by two orders of magnitude the global maximum power, $P_{max}$, simply increased by the

*Corresponding Author e-mail: terry.j.hendricks@jpl.nasa.gov Phone: 1-818-354-4779
Address: 4800 Oak Grove Drive, Pasadena, CA 91109-8099

same fraction, but the normalized power relationship [$P/P_{max}$] demonstrated in Figure 2 stayed constant for a given set of TE materials.

The [$P/P_{max}$] - [$R_{h,th}/R_{c,th}$] relationship exhibits significantly different behavior as it asymptotes to 1 for the two different TE material and couple design cases (Set 1 vs. Set 2). The Set 2 case (dual-segmented design with Skutterudite/Bismuth Telluride materials) exhibited a slower asymptote to 1 requiring larger [$R_{h,th}/R_{c,th}$] values to achieve the global maximum power. This study did not attempt to explain this in detail at the current time, but it is clear the normalized power [$P/P_{max}$] behavior is dependent on the TE materials and couple design as one would expect. More research is needed to characterize this effect completely, but TE system designers and program managers should account for this in future design efforts.

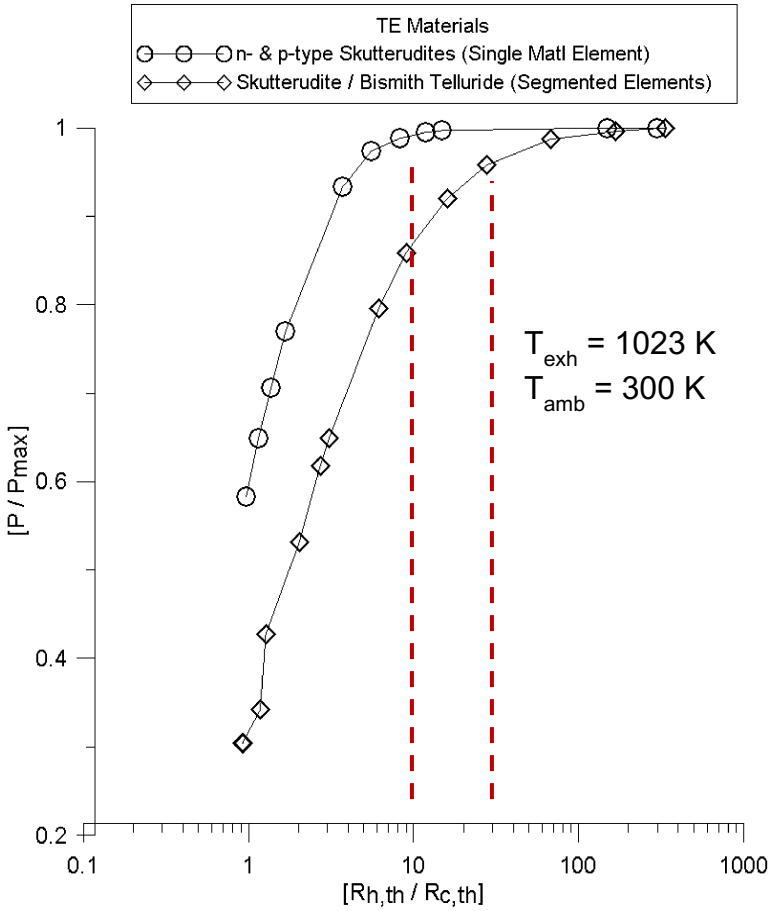


**Figure 3.** [$P/P_{max}$] as Function of [$R_{h,th}/R_{c,th}$] for Set 1 and Set 2 TE Materials and Couple Configurations.

One critical TE system design point that is crystal clear is that to approach the global maximum power condition, [$P/P_{max}$] ≈ 1, the [$R_{h,th}/R_{c,th}$] ratio must be > 10 to 30 depending on the TE materials and couple configuration. This contradicts the conclusion by Yazawa and Shakouri [16] from their simplified, closed-form analysis that a [$R_{h,th}/R_{c,th}$] = 1 condition would achieve a maximum power (or power per area) condition in TE system designs. The results from this investigation show that the power output would be far from the global maximum power point at [$R_{h,th}/R_{c,th}$] = 1, being 40% or even as much as 70% below the global maximum power point depending on the TE materials and couple configuration selected. It is also clear that the [$P/P_{max}$] -

*Corresponding Author e-mail: terry.j.hendricks@jpl.nasa.gov Phone: 1-818-354-4779
Address: 4800 Oak Grove Drive, Pasadena, CA 91109-8099

$[R_{h,th}/R_{c,th}]$ relationship is quite steep and sensitive to $[R_{h,th}/R_{c,th}]$ in the range $1 < [R_{h,th}/R_{c,th}] < 10$ for both TE material sets, thus the penalty on power output is quite severe in this range, which creates enormous implications on TE power system design in all energy recovery applications.

This investigation also simultaneously determined the $[(T_h - T_c)/(T_{exh} - T_{amb)}]$ relationship presented in equation 4 from the information that is available in typical analysis results shown in Figure 2. The $[(T_h - T_c)/(T_{exh} - T_{amb)}]$ value at each power ratio – thermal resistance ratio point in Figure 3 was established. Figure 4 shows $[(T_h - T_c)/(T_{exh} - T_{amb)}]$ as a function of $[R_{h,th}/R_{c,th}]$ for Set 1 TE materials and couple configuration. Figure 4 shows that $[(T_h - T_c)/(T_{exh} - T_{amb)}]$ increases sharply along with $[P/P_{max}]$ as $[R_{h,th}/R_{c,th}]$ increases, ultimate reaching an asymptote value of about 0.48 at the global maximum power condition for Set 1 TE materials and couple configuration. This means that slightly less than ½ of the total environment temperature differential $[T_{exh} - T_{amb}]$ is used across the TE device at the global maximum power condition. The remaining temperature differential is used to drive thermal transport into and out of the TE device at the global maximum power condition. Although not plotted here, $[(T_h - T_c)/(T_{exh} - T_{amb)}]$ - $[R_{h,th}/R_{c,th}]$ relationship for the Set 2 TE materials and couple configuration exhibits the same basic behavior as $[P/P_{max}]$ and $[R_{h,th}/R_{c,th}]$ increase, however in that case $[(T_h - T_c)/(T_{exh} - T_{amb)}]$ asymptotes to about 0.42 at global maximum power conditions. Therefore only about 42% of the total environment temperature differential is used across the TE device at the global maximum power condition. Both of these critical $[(T_h - T_c)/(T_{exh} - T_{amb)}]$* values at global maximum power are below the value of 0.5 found by Yazawa and Shakouri [16] in their system analyses attempting to quantify this ratio. The reason for this is the simplifying assumptions that Yazawa and Shakouri made in their analyses, primarily treating the n-type and p-type TE materials as one, neglecting TE material temperature-dependency, neglecting electrical contact resistance, and neglecting parasitic thermal

*Corresponding Author e-mail: terry.j.hendricks@jpl.nasa.gov Phone: 1-818-354-4779
Address: 4800 Oak Grove Drive, Pasadena, CA 91109-8099

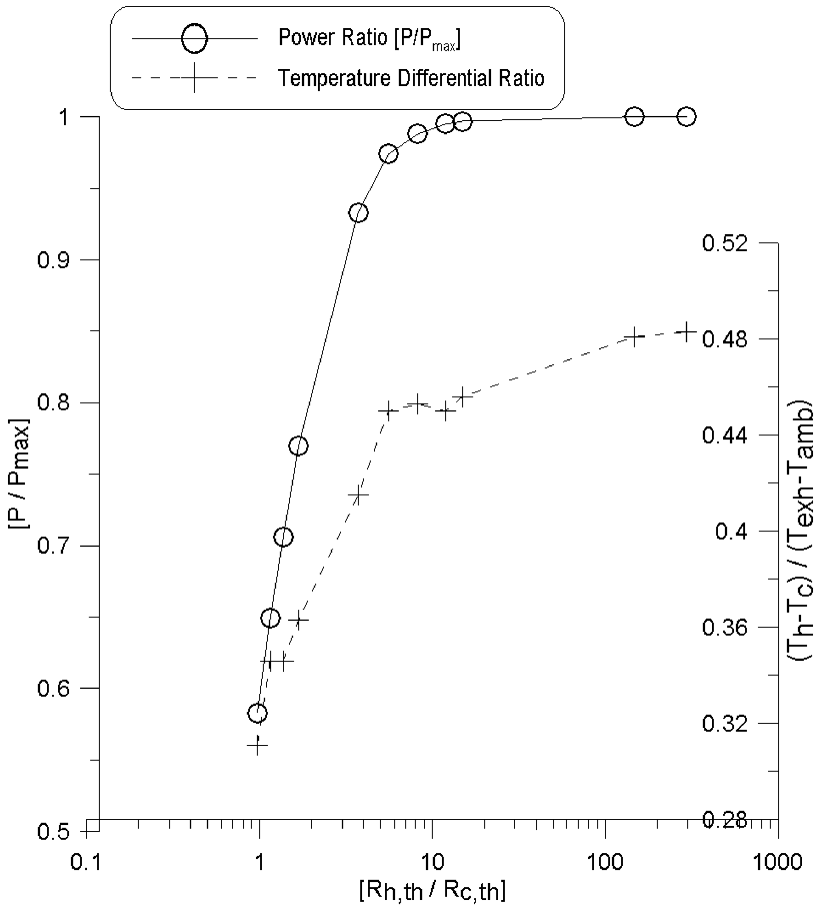


**Figure 4.** $[(T_h - T_c)/(T_{exh} - T_{amb})]$ as a Function of $[R_{h,th}/R_{c,th}]$ for Set 1 TE Materials and Couple Configuration (i.e., Single TE Material Couple Legs).

losses in their TE system analysis. It should be noted that the $[(T_h - T_c)/(T_{exh} - T_{amb})]^* = 0.48$ for the single-material TE couple design (Set 1 TE materials) is reasonably close to the 0.5 that Yazawa and Shakouri did find given all their simplifying assumptions. It should be noted that the reason that the $[(T_h - T_c)/(T_{exh} - T_{amb})]$ values in Figure 4 deviate from a smooth curve is that the temperature search routines in the analyses shown in Figure 2 had a relatively large temperature resolution in an effort to save computational time. It is expected the $[(T_h - T_c)/(T_{exh} - T_{amb})]$ curve would smooth itself as smaller temperature steps were adopted in the search routine.

The curves shown in Figures 3 and 4 also were checked using a different $T_{exh} = 998$ K, which would be consistent with a lower temperature exhaust stream application. The resulting $[P/P_{max}]$ and $[(T_h - T_c)/(T_{exh} - T_{amb})]$ data and curves for this $T_{exh} = 998$ K case were found to be consistent and unwavering with the data exhibited in Figures 3 and 4. This shows the generality of these $[P/P_{max}]$ and $[(T_h - T_c)/(T_{exh} - T_{amb})]$ as a function of $[R_{h,th}/R_{c,th}]$ within this $T_{exh}$ temperature range. More work is recommended to completely verify the expected range of $T_{exh}$ over which these general $[P/P_{max}]$ and $[(T_h - T_c)/(T_{exh} - T_{amb})]$ relationships generally extend, but these results gave every indication they apply across a wide $T_{exh}$ range.

**Effect of reducing $R_{h,th}$**

During the course of this analytic investigation, $[P/P_{max}]$ was characterized for a range of values of $R_{h,th}$ that varied by two orders of magnitude (from ~0.3 K/W to ~0.003 K/W) for both Set 1 and

*Corresponding Author e-mail: terry.j.hendricks@jpl.nasa.gov Phone: 1-818-354-4779
Address: 4800 Oak Grove Drive, Pasadena, CA 91109-8099

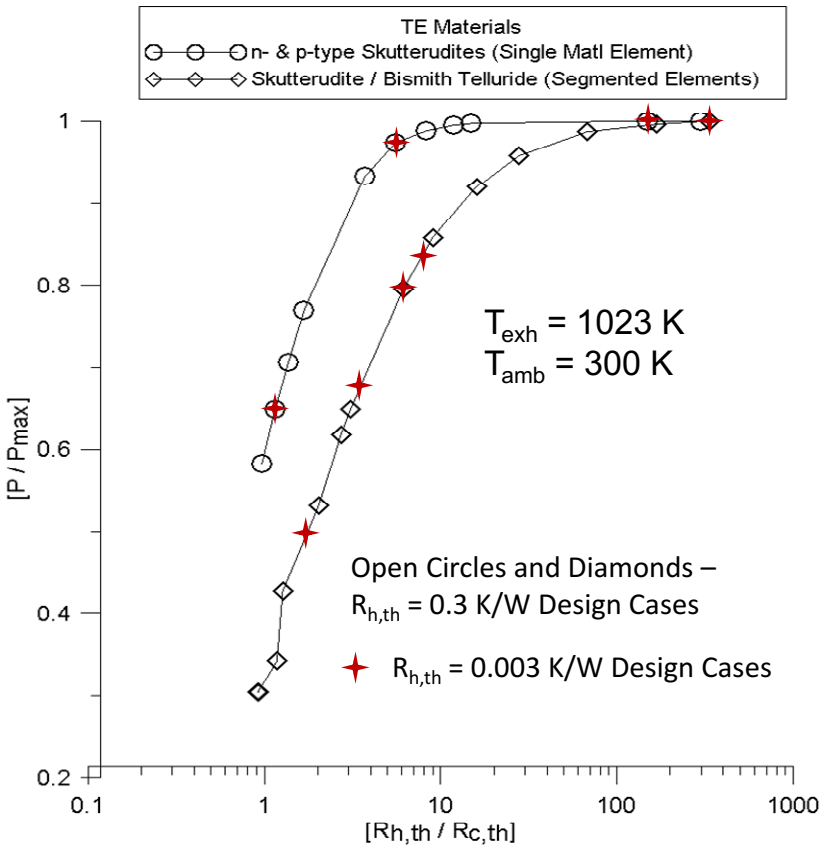


**Figure 5**. $[P/P_{max}]$ as Function of $[R_{h,th}/R_{c,th}]$ for Set 1 and Set 2 TE Materials and Couple Configurations as $R_{h,th}$ Varied From 0.3 K/W to 0.003 K/W. Red Stars Show $R_{h,th}$ = 0.003 K/W Cases.

Set 2 TE materials and couple configurations. Figure 3 and 4 data results were initially created from analyses where $R_{h,th}$ was set at ~0.3 K/W. Figure 5 shows some key $\{[P/P_{max}]$ , $[R_{h,th}/R_{c,th}]\}$ data for cases with $R_{h,th}$ = 0.003 K/W (red stars in Figure 5) superimposed on the original data. This confirmed the steadfast nature of the $[P/P_{max}]$ - $[R_{h,th}/R_{c,th}]$ relationships shown in Figure 3 and 4 for a wide range of $R_{h,th}$ in this study. As $R_{h,th}$ decreased the amount of thermal transfer into the TE device increased proportionally for the same TE device hot-side and cold-side temperature conditions (and therefore same TE device conversion efficiency), thereby increasing the $P_{max}$ proportionally for those consistent conditions. However, the $[P/P_{max}]$ ratios stay constant along the $[P/P_{max}]$ - $[R_{h,th}/R_{c,th}]$ curves shown in Figure 5 as $R_{h,th}$ decreases and increases, thereby the increasing and decreasing the hot-side heat flow, respectively. Therefore, the $[P/P_{max}]$ - $[R_{h,th}/R_{c,th}]$ relationships in Figure 5 remains constant for a given TE material selection and governs the optimum $[R_{h,th}/R_{c,th}]$ selection to achieve maximum possible TE system power conditions for different system designs and configurations applicable to a given waste energy recovery application. More design research is needed with additional TE material sets and couple configurations, but results of this initial investigation clearly demonstrate the behavior and trends to expect with other TE materials and couple configurations.

## Electrical contact resistance effects

*Corresponding Author e-mail: terry.j.hendricks@jpl.nasa.gov Phone: 1-818-354-4779
Address: 4800 Oak Grove Drive, Pasadena, CA 91109-8099

The electrical contact resistance internal to the TE devices can have a significant impact on TE system power output because of parasitic joule heating losses. Therefore the effects of electrical contact resistance at the n-type and p-type TE junctions on the $[P/P_{max}]$ - $[R_{h,th}/R_{c,th}]$ relationships also was investigated using the TE system analysis shown in Figures 1 and 2. It was important to understand if there was any cross non-linear interdependencies with thermal resistance effects which would impact or modify the power - thermal resistance behavior discussed above. The power output, P, at the MPME point in Figure 2 was characterized for the same values of $R_{h,th}$ , $R_{c,th}$, and $[R_{h,th}/R_{c,th}]$ ratios, two material set selections, and with the TE device electrical contact resistance doubled in each design case. The MPME power output was once again normalized against the $P_{max}$ case identified in the TE system analyses using double (i.e., 2 times) the electrical contact resistance used in results shown in Figure 3. Figure 6 illustrates the analysis results for these design cases compared to the baseline cases in Figure 3. The results clearly demonstrate that once again the $[P/P_{max}]$ - $[R_{h,th}/R_{c,th}]$ relationships remain consistent as TE device n-type and p-type electrical contact resistances are increased. Once again all the TE device power levels do indeed decrease, including $P_{max}$, but they do so proportionally such that the $[P/P_{max}]$ ratios remain the same along the $[P/P_{max}]$ - $[R_{h,th}/R_{c,th}]$ curves. This once again demonstrates the comprehensive generality of the $[P/P_{max}]$ - $[R_{h,th}/R_{c,th}]$ relationships and that optimum $[R_{h,th}/R_{c,th}]$ values to achieve the global maximum power condition remain constant as this critically important TE device parameter is varied. It is fully expected that these relationships would also hold even if the device electrical contact resistance varied across a much broader range. This conclusion is quite critical because it is often hard to control and manage the n-type and p- type electrical contact resistances in various TE device designs, either at beginning-of-design-life or as the TE devices mature and age under operating conditions. This has tremendous implications on identifying and achieving global maximum power conditions in TE energy recovery system designs in industrial and transportation applications.

*Corresponding Author e-mail: terry.j.hendricks@jpl.nasa.gov Phone: 1-818-354-4779
Address: 4800 Oak Grove Drive, Pasadena, CA 91109-8099

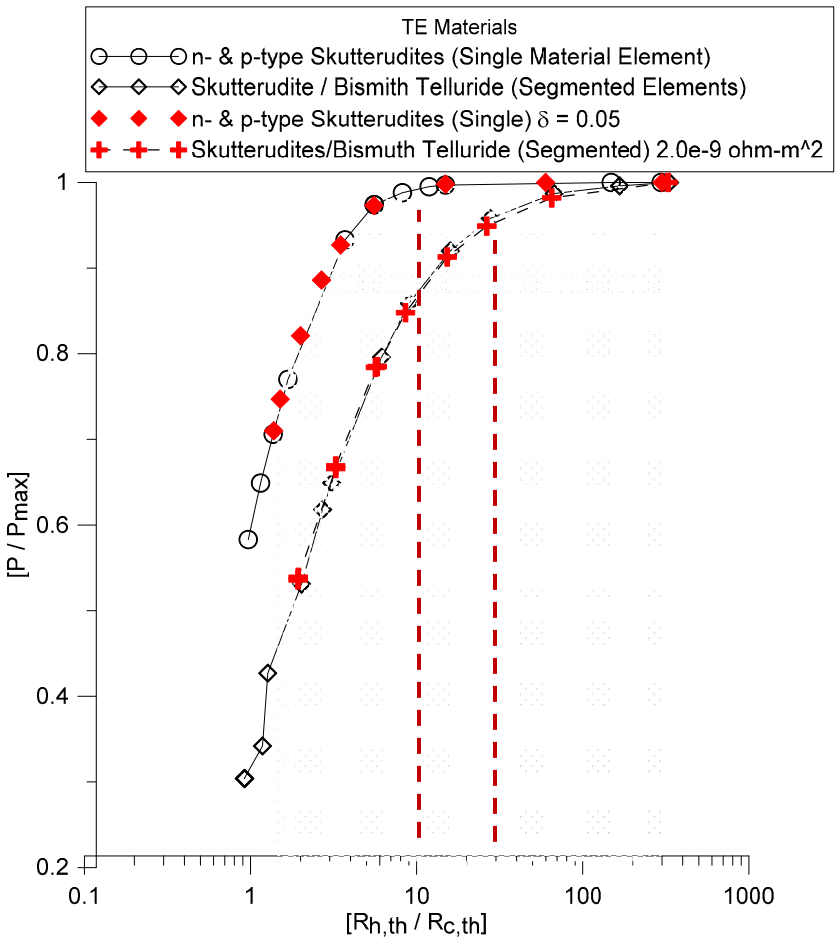


**Figure 6.** $[P/P_{max}]$ as Function of $[R_{h,th}/R_{c,th}]$ for Set 1 and Set 2 TE Materials and Couple Configurations With Double the Electrical Contact Resistance in the TE Devices.

## Parasitic thermal loss effects

The TE device design and power output is also dramatically affected by parasitic thermal losses within the TE power and thermal system, thermal losses decreasing power output just as electrical contact resistances do. The system analysis presented by Hendricks et al. [11, 12, and 14] allows one to include the effects of these parasitic thermal losses on the TE device and system design and power output. The system study results shown in Figures 3, 5, and 6 were performed for parasitic thermal losses modeled at 15% of the TE device hot-side heat flows. It was important to understand the impact of these thermal losses and if there was any cross non-linear interdependencies between parasitic thermal loss and thermal resistance effects which would impact or modify the power - thermal resistance behavior discussed above. Therefore the effects of parasitic thermal losses on the $[P/P_{max}]$ - $[R_{h,th}/R_{c,th}]$ relationships also was investigated using the TE system analysis shown in Figures 1 and 2. The power output, P, at the MPME point in Figure 2 was characterized for the same values of $R_{h,th}$ , $R_{c,th}$, and $[R_{h,th}/R_{c,th}]$ ratios, two material set selections, and with the parasitic thermal losses driven to zero (i.e., an idealized extreme case) in each design case. The MPME power output was once again normalized against the $P_{max}$ case identified in the TE system analyses using this zero thermal loss condition. Figure 7 illustrates the $[P/P_{max}]$ analysis results for these design cases compared to the baseline cases in Figures 3 and 6.

*Corresponding Author e-mail: terry.j.hendricks@jpl.nasa.gov Phone: 1-818-354-4779
Address: 4800 Oak Grove Drive, Pasadena, CA 91109-8099

Once again $[P/P_{max}]$ - $[R_{h,th}/R_{c,th}]$ relationships track very closely to the baseline cases in Figures 3 and 6 and demonstrate the comprehensive generality of these relationships even when comparing between a realistic parasitic thermal loss case and the idealized, extreme zero-loss case. The optimum $[R_{h,th}/R_{c,th}]$ values to achieve the global maximum power condition remain consistent with previous conclusions ($[R_{h,th}/R_{c,th}]_{opt}$ > 10 to 30), thereby emphasizing that there are no strong cross non-linear interdependencies from parasitic thermal loss effects. This steadfast, strongly consistent relationship $[P/P_{max}]$ - $[R_{h,th}/R_{c,th}]$ relationship once again shows its quite strong sensitivity to $[R_{h,th}/R_{c,th}]$ in the range $1 < [R_{h,th}/R_{c,th}] < 10$ for both TE material sets and each design parameter investigated. It is worth reiterating the severe penalty on power output in this range producing enormous implications on TE power system design in all energy recovery applications.

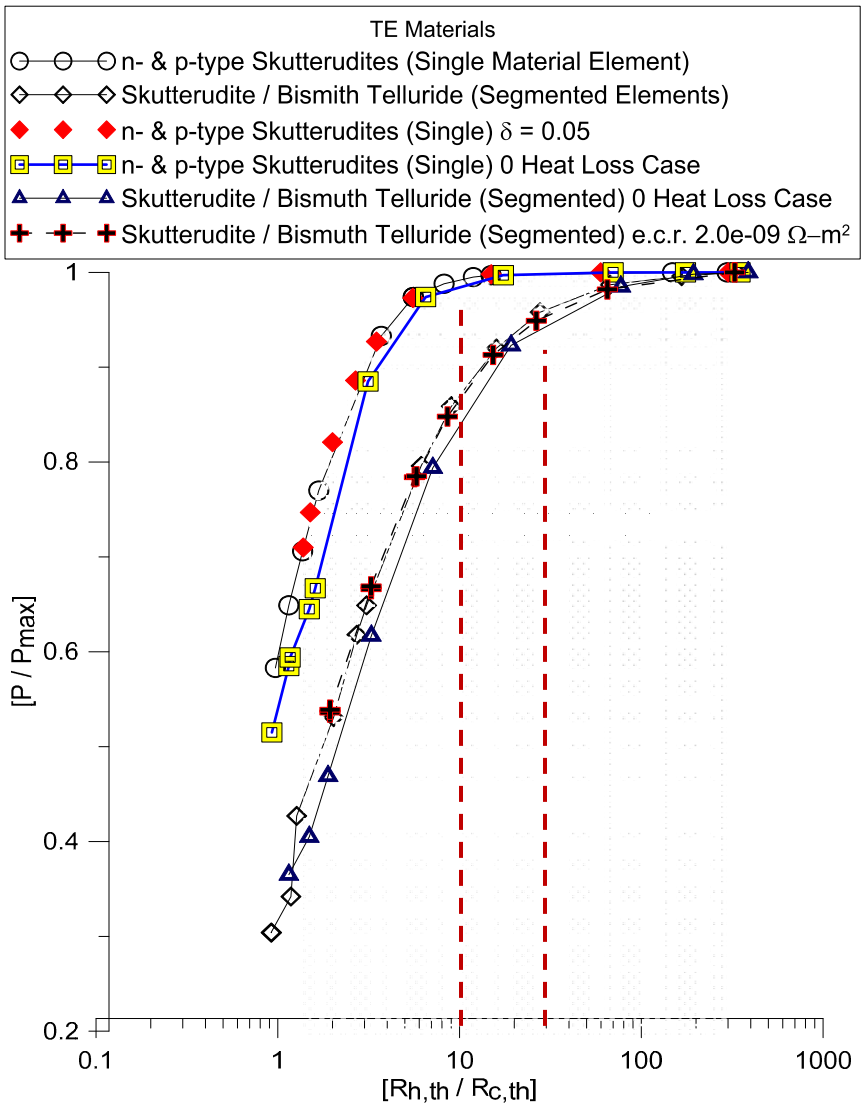


**Figure 7.** $[P/P_{max}]$ as Function of $[R_{h,th}/R_{c,th}]$ for Set 1 and Set 2 TE Materials and Couple Configurations With Zero Parasitic Thermal Losses in the TE Devices.

Figure 8 displays the $[P/P_{max}]$ - $[R_{h,th}/R_{c,th}]$ analysis results for Set 3 TE materials (bismuth telluride materials) for analysis cases where $T_{exh}$ = 623 K and 648 K with $T_{amb}$ = 300 K. The

*Corresponding Author e-mail: terry.j.hendricks@jpl.nasa.gov Phone: 1-818-354-4779
Address: 4800 Oak Grove Drive, Pasadena, CA 91109-8099

$[P/P_{max}]$ - $[R_{h,th}/R_{c,th}]$ relationship shown in Figure 8 is remarkably similar to that shown in Figures 3, 5, 6, and 7 for other TE material combinations and temperatures. In this case, the maximum power is realized at $[R_{h,th}/R_{c,th}]_{opt} > 20$, strikingly similar to the earlier conclusion $[R_{h,th}/R_{c,th}]_{opt}$ >10-30 for TE material sets #1 and #2. The major early conclusion from this work is therefore that the TE material selection does not strongly impact the optimum $[R_{h,th}/R_{c,th}]$ which produces maximum power conditions in TE energy recovery systems.

The optimum $[R_{h,th}/R_{c,th}]$ (>10-30) developed in this work aligns with and is explained by the fundamental physics of TE device design and operation. A large value $[R_{h,th}/R_{c,th}]$ implies that $R_{c,th}$ is small and approaching 0 for any value of $R_{h,th}$. This essentially drives the cold-side temperature, $T_c$, to approach the ambient temperature, $T_{amb}$, in any given TE energy recovery application, resulting in the largest temperature differential $(T_h - T_c)$ across the TE device for any given $R_{h,th}$. The TE power output is proportional to the $(T_h - T_c)^2$, therefore it is maximized as $R_{c,th}$ decreases and approaches 0 and $(T_h - T_c)$ maximizes for any given $R_{h,th}$ in energy recovery applications with

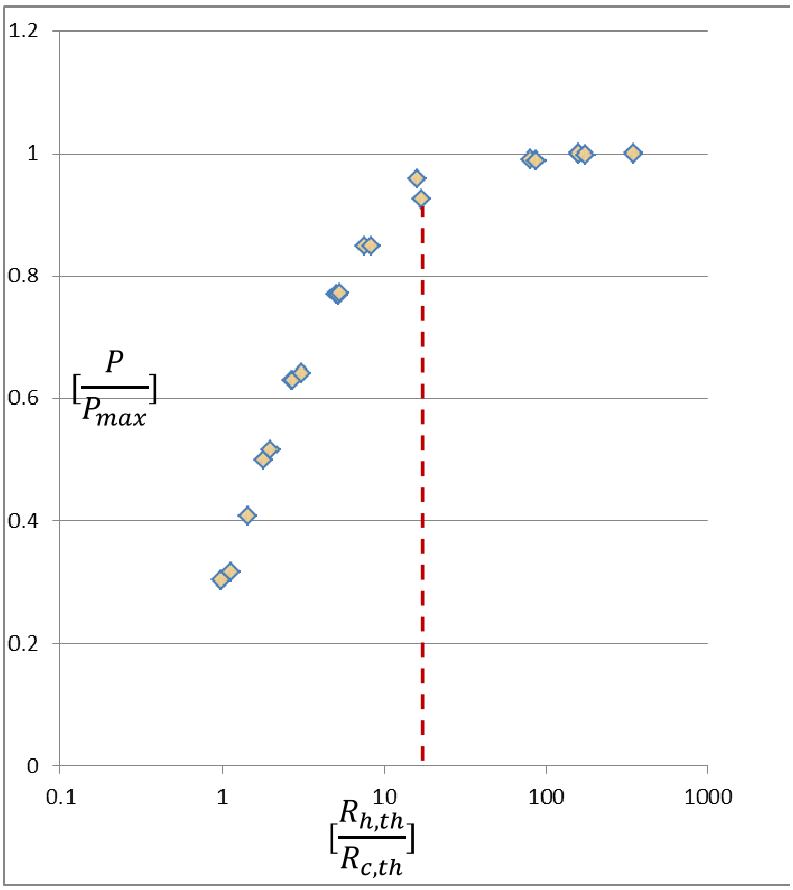


**Figure 8** - $[P/P_{max}]$ as Function of $[R_{h,th}/R_{c,th}]$ for p-type / n-type Bismuth Telluride TE Materials (Set 3) in a Single-Material-Leg Couple Design for $T_{exh}$ = 623 K and 648 K with $T_{amb}$ = 300 K.

an overall temperature differential $(T_{exh} - T_{amb})$ to work with. This effect was seen experimentally in work by Wang et al. [22] where TE system power did indeed increase as $T_c$ approached the cooling fluid temperatures (representing $T_{amb}$ in this analysis). It should be re-iterated that all the investigation results discussed here and the data in Figures 3, 5, 6, 7 and 8 clearly show that power output does not maximize at $[R_{h,th}/R_{c,th}] = 1$ as implied by Yazawa and Shakouri [16], in fact power

*Corresponding Author e-mail: terry.j.hendricks@jpl.nasa.gov Phone: 1-818-354-4779
Address: 4800 Oak Grove Drive, Pasadena, CA 91109-8099

output is far from maximum conditions at this [$R_{h,th}/R_{c,th}$] condition. Furthermore, there is no analogy with electric circuit design as these are two fundamentally different physical phenomena.

The [$P/P_{max}$] - [$R_{h,th}/R_{c,th}$] relationships shown in Figures 3, 5, 6, 7 and 8 illustrate and define the fundamental connection between the TE system power output and the thermal system design, and govern the optimum system design conditions. The over-arching conclusion from this work is clearly that to achieve global maximum power conditions there are two system design optimization criteria that must be met; 1) the thermoelectric design criteria for maximizing TE system power output [Rowe, 13] with integrated heat exchanger performance demonstrated in Figure 2 and in Hendricks and Crane [14], and 2) the system thermal resistance ratio criteria ($[R_{h,th}/R_{c,th}]_{opt} > 10$ to 30) demonstrated in Figures 3, 5, 6, 7 and 8. The [$P/P_{max}$] - [$R_{h,th}/R_{c,th}$] relationships shown in Figures 3, 5, 6, and 7 also define the fundamental relationship between the thermal system design, quantified by $R_{h,th}$ and $R_{c,th}$, and the TE system electrical power output. The ramifications of these relationships and conclusion on TE energy recovery systems and their design optimization for industrial and transportation-related applications are far-reaching. Certainly more work needs to be done to crystallize this discovery for additional TE materials and couple configurations, but the results of this investigation clearly demonstrate the behavior and trends.

Table I shows the optimum $[(T_h - T_c)/(T_{exh} - T_{amb})]^*$ values at maximum power generation conditions for skutterudite-alone materials and couples (Set 1), skutterudite/bismuth telluride segmented materials and couples (Set 2), and bismuth-telluride-alone materials and couples (Set 3) in Figures 3, 5, 6, 7, and 8. These results show that the optimum $[(T_h - T_c)/(T_{exh} - T_{amb})]^*$ values at maximum power depend strongly on the TE materials that one selects, and most importantly their corresponding specific temperature-dependent TE property behavior, in any given TE energy recovery design and application. It is critical to recognize the role that the temperature-dependent TE property behavior plays in establishing optimum TE device temperature conditions and differentials, and TE proportion of overall available ($T_{exh}$-$T_{amb}$) differential, at maximum power. In each case, a significant portion of the overall available ($T_{exh}$-$T_{amb}$) differential is taken across the heat exchanger systems to effectively drive thermal energy into and out of the TE conversion devices.

**Table I** – Optimum TE Temperature Differential Ratios Maximizing Power Generation for Selected TE Materials

| TE Materials and Couple Configuration | Bismuth Telluride Alone (Set 3) | Skutterudites/ Bismuth Telluride Segmented (Set 2) | Skutterudites Alone (Set 1) | Yazawa & Shakouri (2012) |
|---|---|---|---|---|
| $[(T_h - T_c)/(T_{exh} - T_{amb})]^*$ | 0.37-0.38 | 0.42 | 0.48 | 0.5 |

**Special case – $R_{h,th} \rightarrow 0$**

There is a theoretically-possible, but in reality impossible, special-case condition to consider in addressing this question of determining $(R_{h,th}/R_{c,th})_{opt}$. This is the case where $R_{h,th} \rightarrow 0$, which would indeed essentially and simultaneously drive $T_h$ toward $T_{exh}$, generate the largest hot-side thermal transfer into the TE device, and increase $(T_h - T_c)$ which increases the TE system conversion efficiency and power output for a given $(T_{exh} - T_{amb})$ environment. In this case the

*Corresponding Author e-mail: terry.j.hendricks@jpl.nasa.gov Phone: 1-818-354-4779
Address: 4800 Oak Grove Drive, Pasadena, CA 91109-8099

global maximum power would be created once again under a condition where $R_{c,th} \rightarrow 0$, thereby forcing $T_c$ toward $T_{amb}$ and creating the absolute maximum TE device temperature differential $(T_h - T_c)_{max} = (T_{exh} - T_{amb})$, and globally maximizing TE power output because of its $(T_h - T_c)^2$ dependency. This would create a mathematical condition where TE system power output is maximized by $[R_{h,th}/R_{c,th}] \rightarrow 0/0$, where this mathematically-undetermined quantity could approach 1 depending on how $R_{h,th}$ and $R_{c,th}$ approach 0 in the case considered. This is really an abstract theoretical exercise in that neither of these thermal resistance conditions can be achieved in reality, but it does demonstrate a special case where $[R_{h,th}/R_{c,th}] \rightarrow 1$ could create a global maximum TE power output condition for a given waste energy recovery application with a $(T_{exh} - T_{amb})$ environment. It is actually the Carnot condition referred to by Yazawa and Shakouri [16] in their work on this subject.

## CONCLUSIONS

This work demonstrated a comprehensive, unwavering generality of the $[P/P_{max}]$ - $[R_{h,th}/R_{c,th}]$ relationships shown in equation 3 through the analysis results presented in Figures 3, 5, 6, 7, and 8 for a wide variation in key TE design parameters ($R_{h,th}$, electrical contact resistance, parasitic thermal loss conditions, and $T_{exh}$). They illustrate and define the fundamental connection between the thermal system design, specified by $R_{h,th}$ and $R_{c,th}$, and TE system electrical power output and dictate the optimum system design conditions. The strong, steadfast consistency in these relationships demonstrated that achieving global maximum power conditions in a TE system design requires that two system design optimization criteria must be met: 1) optimum thermoelectric design criteria for maximizing TE system power output [See Rowe et al., 13] with integrated heat exchanger performance demonstrated in Figure 2 [Hendricks and Crane, 14, Hendricks, 15], and 2) optimum selection of system hot-side to cold-side thermal resistance ratio $[R_{h,th}/R_{c,th}]_{opt}$ demonstrated in Figures 3, 5, 6, 7, and 8. The optimum thermal resistance condition to maximize TE system power output was established as:

$$(R_{h,th} / R_{c,th})_{opt} > 10 \text{ to } 30 \qquad (5)$$

This optimum $[R_{h,th}/R_{c,th}]$ condition aligns with and is explained by the fundamental physics of TE device design and operation. A large value $[R_{h,th}/R_{c,th}]$ essentially drives the cold-side temperature, $T_c$, to approach the ambient temperature, $T_{amb}$, in any given TE energy recovery application, resulting in the largest temperature differential $(T_h - T_c)$ across the TE device for any given $R_{h,th}$, thereby maximizing TE power output through its fundamental $(T_h - T_c)^2$ dependence. $(R_{h,th}/R_{c,th}) = 1$ does not maximize power output. In fact, the $[P/P_{max}]$ - $[R_{h,th}/R_{c,th}]$ relationship is strongly sensitive to $[R_{h,th}/R_{c,th}]$ in the range $1 < [R_{h,th}/R_{c,th}] < 10$ and creates a severe penalty on power output in this range and enormous implications on TE power system designs in all energy recovery applications.

The $[(T_h - T_c)/(T_{exh} - T_{amb})]$ - $[R_{h,th}/R_{c,th}]$ relationships given in equation 4 for the Set 1 and Set 2 TE materials and couple configuration exhibited similar basic behavior (shown in Figure 4) increasing in a predictable, asymptotic manner as $(P/P_{max})$ approaches 1. These relationships demonstrated the same comprehensive, steadfast generality that the $[P/P_{max}]$ - $[R_{h,th}/R_{c,th}]$ relationships show when $R_{h,th}$, electrical contact resistance and parasitic thermal losses were varied. $[(T_h - T_c)/(T_{exh} - T_{amb})]$ ultimately reaches its asymptotic value of about $[(T_h - T_c)/(T_{exh} - T_{amb})]^* = 0.48$ at the global maximum power condition for Set 1 TE materials and the single-material couple configuration. In the case of Set 2 TE materials and the segmented couple configuration, this

*Corresponding Author e-mail: terry.j.hendricks@jpl.nasa.gov Phone: 1-818-354-4779
Address: 4800 Oak Grove Drive, Pasadena, CA 91109-8099

temperature ratio reaches an asymptotic value of about $[(T_h - T_c)/(T_{exh} - T_{amb})]^* = 0.42$ at global maximum power conditions. In the case of Set 3 TE materials and the single-material couple configuration, this temperature ratio reaches an asymptotic value of about $[(T_h - T_c)/(T_{exh} - T_{amb})]^* = 0.37\text{-}38$ at global maximum power conditions. The essential $[(T_h - T_c)/(T_{exh} - T_{amb})]^*$ value at global maximum power conditions is therefore quite dependent on TE materials, TE property temperature dependencies, and TE couple configuration used in the TE device design. This result also implies that less than ½ of the total environment temperature differential $[T_{exh} - T_{amb}]$ is used across the TE device at the global maximum power condition, with the remaining temperature differential used to drive thermal transport into and out of the TE device at the global maximum power condition.

The ramifications of these conclusions on TE energy recovery systems and their design optimization for industrial and transportation-related applications are far-reaching. This has tremendous implications on identifying and achieving global maximum power conditions in TE energy recovery system designs for these applications, quantifying simultaneous system-level TE and thermal design requirements, developing TE system testing requirements and performance validation expectations, and developing optimum system configurations that can allow TE energy recovery systems to achieve their full potential and promise. More research work is recommended to expand and crystalize these results into a unified design-rule hierarchy for additional TE materials and couple configurations applicable to a wide spectrum of TE energy recovery systems.

## REFERENCES


1. *Transportation Energy Data Book,* 2010, Edition 29, U.S. Department of Energy, Office of Energy Efficiency and Renewable Energy, Vehicles Technology Program. ORNL-6985, Oak Ridge National Laboratory, Oak Ridge, Tennessee. http://cta.ornl.gov/data/index.shtml.
2. *Energy Use, Loss and Opportunities Analysis: U.S. Manufacturing and Mining.* 2004, U.S. Department of Energy, Office of Energy Efficiency and Renewable Energy, Industrial Technologies Program, Energetics, Inc. & E3M, Inc.
3. Hendricks, T.J. and Choate, W.T., 2006, "Engineering Scoping Study of Thermoelectric Generator Packages for Industrial Waste Heat Recovery," U.S. Department of Energy, Industrial Technology Program, http://www.eere.energy.gov/industry/imf/analysis.html.
4. Hendricks, T.J., Hogan, T.P., Case, E.D., Cauchy, C.J., Karri, N.K., D'Angelo, J., Wu, C.-I., Morrison, A.Q., Ren, F., 2009. "Advanced Soldier-Based Thermoelectric Power Systems Using Battlefield Heat Sources," in Energy Harvesting--From Fundamentals to Devices, edited by H. Radousky, J. Holbery, L. Lewis, F. Schmidt (Mater. Res. Soc. Symp. Proc. Volume 1218E, Warrendale, PA, 2010), Paper ID # 1218-Z07-02. (*Proceedings of the Materials Research Society 2009 Fall Meeting*, Symposium Z, Paper ID # 1218-Z07-02, Boston, MA, 2009.)
5. Hendricks, T.J., Karri, N.K., Hogan, T.P., and Cauchy, C.J., 2010, "New Thermoelectric Materials and New System-Level Perspectives Using Battlefield Heat Sources for Battery Recharging," *Proceedings of the 44th Power Sources Conference*, Institute of Electrical and Electronic Engineers Power Sources Publication, Technical Paper #28.2, pp. 609-612.
6. Crane, D.T., 2011 "An Introduction to System Level Steady-State and Transient Modeling and Optimization of High Power Density Thermoelectric Generator Devices Made of Segmented Thermoelectric Elements", *Journal of Electronic Materials*, **40** (5), 561-569.



*Corresponding Author e-mail: terry.j.hendricks@jpl.nasa.gov Phone: 1-818-354-4779
Address: 4800 Oak Grove Drive, Pasadena, CA 91109-8099

7. Crane, D.T. and Bell, L.E., 2009, "Design to Maximize Performance of a Thermoelectric Power Generator With a Dynamic Thermal Power Source," *Journal of Energy Resources Technology*, **131**:012401-1 to 8.
8. Crane, D.T. and Jackson, G.S., 2004, "Optimization of Cross Flow Heat Exchangers for Thermoelectric Waste Heat Recovery," *International Journal of Energy Conversion and Management*, **45**(9-10): 1565-1582.
9. Crane, D.T., LaGrandeur, J.W., and Bell, L.E., 2010, "Progress Report on BSST Led, U.S. DOE Automotive Waste Heat Recovery Program," *Journal of Electronic Materials*, **39**(9): 2142-2148.
10. Salvador, J.R., Cho, J.Y., Ye, Z., Moczygemba, J.E., Thompson, A.J., Sharp, J.W., König, J.D., Maloney, R., Thompson, T., Sakamoto, J., Wang, H., Wereszczak, A.A., Meisner, G.P., 2013, "Thermal to Electrical Energy Conversion of Skutterudite-Based Thermoelectric Modules", *Journal of Electronic Materials* , **42** (7), 1389-1399.
11. Hendricks, T.J., Karri, N.K., Hogan, T.P. & Cauchy, C.J., 2013, "New Perspectives in Thermoelectric Energy Recovery System Design Optimization", *Journal of Electronic Materials,* **42** (7), DOI 10.1007/s11664-012-2406-x, 1725-1736.
12. Hendricks, T.J., 2007, "Thermal System Interactions in Optimizing Advanced Thermoelectric Energy Recovery Systems", *Journal of Energy Resources Technology*, **129** (3), American Society of Mechanical Engineers, New York, 223–231.
13. Rowe, D.M., Ed. 2006, Thermoelectrics Handbook Macro to Nano, Chapter 2, CRC Press Taylor and Francis Group, Boca Raton, FL.
14. Hendricks, T.J. and Crane, D., T., 2012,"Thermoelectric Energy Recovery Systems: Thermal, Thermoelectric and Structural Considerations", Book 2, Section 3, Chapter 22, Thermoelectrics and Its Energy Harvesting – Modules, Systems, and Applications in Thermoelectrics, Rowe, D.M., Ed., CRC Press Taylor and Francis Group, Boca Raton, FL.
15. Hendricks, T.J., 2014, "Energy Harvesting: Thermoelectric and Microsystems Perspectives and Opportunities", Chapter 3, Energy Harvesting with Functional Materials and Microsystems, Bhaskaran, M., Sriram, S., and Iniewski, K., Eds., CRC Press Taylor & Francis Group, Boca Raton, FL.
16. Yazawa, K. and Shakouri, A. 2012, "Optimization of Power and Efficiency of Thermoelectric Devices with Asymmetric Thermal Contacts", *Journal of Applied Physics*, **111**, 024509, DOI 10.1063/1.3679544.
17. Fleurial, J.-P., Caillat, T., and Borshchevsky, A., 1997, "Skutterudites: An Update", *Proceedings of the XVI International Conference on Thermoelectrics*, Dresden, Germany.
18. Biswas, K., Good, M.S., Roberts, K.C., Subramanian, M.A., Hendricks, T.J., 2011, "Thermoelectric and Structural Properties of High-Performance In-Based Skutterudites for High-Temperature Energy Recovery", *Journal of Materials Research-Focus Issue: Advances in Thermoelectric Materials,* JMR-2010-0700, Materials Research Society, Warrendale, PA.
19. Li, H., Tang, X., Zhang, Q., and Uher, C., 2009, "High-Performance $In_xCe_yCo_4Sb_{12}$ Thermoelectric Materials With In Situ Forming Nanostructured InSb Phase", *Applied Physics Letters*, **94**, 102144, doi: 10.1063/1.3099804, AIP Publishing.
20. He, T., Chen, J., Rosenfeld, H.D., and Subramanian, M.A., 2006, "Thermoelectric properties of indium-filled skutterudites", *Chem. Mater.* **18**, 759.

*Corresponding Author e-mail: terry.j.hendricks@jpl.nasa.gov Phone: 1-818-354-4779
Address: 4800 Oak Grove Drive, Pasadena, CA 91109-8099

21. Rowe, D.M., Ed. 2006, Thermoelectrics Handbook Macro to Nano, Chapter 27, CRC Press Taylor and Francis Group, Boca Raton, FL.
22. Wang, H., Hendricks, T.J., Krishnan, S., Peterson, R.B., 2011, "Experimental Verification of Thermally Activated Power and Cooling System Using Hybrid Thermoelectric, Organic Rankine Cycle and Vapor Compression Cycle", *Proceedings of the 9th Annual International Energy Conversion Engineering Conference*, San Diego, CA, Paper #AIAA 2011-5983, American Institute of Aeronautics and Astronautics.

*Corresponding Author e-mail: terry.j.hendricks@jpl.nasa.gov Phone: 1-818-354-4779
Address: 4800 Oak Grove Drive, Pasadena, CA 91109-8099